Unified Analysis of Internal Flowfield in an Integrated Rocket Ramjet Engine. I: Transition from Rocket Booster to Ramjet Sustainer

Hong-Gye Sung[1] and Vigor Yang[2]

Abstract: A comprehensive numerical analysis was conducted to study the internal flow development in an integrated rocket-ramjet (IRR) propulsion system. The study consists of two parts: transition from the rocket booster to the ramjet sustainer and combustion dynamics during ramjet operation. The physical model of concern includes the entire IRR flow path, extending from the leading edge of the inlet center body through the exhaust nozzle. The theoretical formulation is based on the Farve-averaged conservation equations of mass, momentum, energy, and species concentration in axisymmetric coordinates and accommodates finite-rate chemical kinetics and variable thermophysical properties. Turbulence closure is achieved using a low-Reynolds-number κ-ε two-equation model. The governing equations are solved numerically by means of a finite-volume preconditioned flux-differencing scheme capable of treating a chemically reacting flow over a wide range of Mach numbers. Various important physiochemical processes involved in the transition from the booster to the sustainer phase are investigated systemically. Emphasis is placed on the flow interactions between the inlet diffuser and combustor. The effects of operation timing on the flow evolution, fuel spread, ignition, and flame development are studied. **DOI: 10.1061/(ASCE)AS.1943-5525.0000255.**

Author keywords: Integrated rocket ramjet engine; Ignition transients; Supersonic aerodynamics.

Introduction

An integrated rocket-ramjet (IRR) engine combines a rocket booster and a ramjet sustainer into a single propulsion unit with a common combustor (Fig. 1). Such an engine features a much more compact configuration than earlier systems having a tandem booster rocket that is jettisoned after propellant burnout (Fry 2004; Myers 1984; Waltrup et al. 2002). The large difference in the chamber operating pressure between the rocket and the ramjet phase poses a major IRR development challenge, which can be solved by using a booster nozzle that is ejected after the boost phase. A booster nozzle, however, creates additional reliability problems, such as the dynamic impact of the nozzle ejection on the vehicle and the increase in the time delay from the rocket to the ramjet phase. A nozzleless booster, using the propellant grain as a nozzle, has been used to circumvent the difficulties inherent in an ejectable nozzle (Waltrup et al. 2002; Zarlingo 1988). During the booster phase, the combustor functions as a conventional rocket combustor, closed at the forward end, with a suitable nozzle formed by the propellant grain at the aft end, as shown schematically in Fig. 1. After the transition to the sustainer phase, the chamber reconfigures itself for ramjet operation, open at the forward end to allow the ram air to enter the combustor, with a large-throat nozzle at the aft end. The port cover, which seals the upstream end of the chamber, is ruptured at the end of the boost phase to facilitate the ramjet operation. After the tail-off of the booster thrust, the drag force acting on the airframe causes the vehicle to rapidly lose its forward speed, typically at a rate on the order of Mach 0.1 per second (Myers 1984). Hence, the transition to ramjet takeover must be accomplished quickly in a timely fashion. When the pressure in the booster combustor decays to a value at which the positive vehicle acceleration approaches zero, the inlet port cover separation mechanism is activated. The port cover is forced into the combustor when the inlet ram air pressure exceeds the residual chamber pressure and is then expelled to the ambient environment through the ramjet nozzle. Reliable ignition and robust burning of the ramjet fuel during this transient phase are critical engine development issues.

Extensive research has been conducted to explore the internal flowfields in ramjet engines, especially in the areas of inlet aerodynamics (Barber et al. 2009; Bemdot et al. 1984; Bogar et al. 1985; Hsieh et al. 1987; Lu and Jain 1998; Oh et al. 2005; Yang and Culick 1985), combustion chamber dynamics (Matveev and Culick 2003; Menon and Jou 1991; Ristori et al. 2003; Webster 1989; Yang and Culick 1986), and active control of flow oscillations (Fung et al. 1991; Fung and Yang 1992). Most of these studies treat either the inlet or the combustor individually. The interactions between the two subsystems have not yet been thoroughly explored, despite the significance of their coupling effects in determining the overall engine dynamics (Hsieh and Yang 1997a). Furthermore, only limited efforts have been devoted to liquid-fueled systems with practical configurations. The purpose of the present work is to conduct a unified analysis of the internal flow development in the entire engine, from the freestream upstream of the inlet center body through the exhaust nozzle. The study consists of two parts: transition from the booster to the ramjet sustainer and flow dynamics in the ramjet phase. Various physiochemical processes and mechanisms dictating the engine internal dynamics are examined systematically. The present paper is organized as follows. The theoretical formulation and numerical treatment of unsteady chemically reacting flows in axisymmetric coordinates are summarized. The flow

[1]Professor, School of Aerospace and Mechanical Engineering, Korea Aerospace Univ., Geonggi 200-1, South Korea.

[2]Professor, School of Aerospace Engineering, Georgia Institute of Technology, Atlanta, GA 30332-0150 (corresponding author). E-mail: vigor@gatech.edu

Note. This manuscript was submitted on November 18, 2011; approved on May 15, 2012; published online on May 18, 2012. Discussion period open until August 1, 2014; separate discussions must be submitted for individual papers. This paper is part of the ***Journal of Aerospace Engineering***, Vol. 27, No. 2, March 1, 2014. ©ASCE, ISSN 0893-1321/2014/2-390–397/$25.00.

J. Aerosp. Eng. 2014.27:390-397.

transients from the booster to the sustainer phase are presented in the section, "Flow Transients from Booster to Sustainer." The situation with the inlet port cover in place is also considered, to provide a more complete description. The ignition transients after the removal of the port cover are treated. The phenomena of fuel injection, mixing of reactants, ignition, and flame evolution in the chamber are examined.

Theoretical Formulation and Numerical Treatment

Governing Equations

The physical model of concern includes the entire engine flowpath, as shown in Fig. 2, extending from the freestream in front of the inlet to the exit of the exhaust nozzle. The formulation is based on the Favre-averaged conservation laws in axisymmetric coordinates and accommodates finite-rate chemical kinetics and variable thermophysical properties for a multicomponent system. The governing equations of mass, momentum, energy, and species concentration take the following form:

$$\frac{\partial \mathbf{Q}}{\partial t} + \frac{\partial(\mathbf{E} - \mathbf{E}_v)}{\partial x} + \frac{\partial(\mathbf{F} - \mathbf{F}_v)}{\partial y} = \mathbf{H} \tag{1}$$

where $\mathbf{E}_v$ and $\mathbf{F}_v$ = diffusion flux vectors; and $\mathbf{H}$ = source term vector. The conserved variable vector $\mathbf{Q}$ and inviscid flux vectors ($\mathbf{E}$, $\mathbf{F}$) are defined as

$$\mathbf{Q} = y\left[\overline{\rho}, \quad \overline{\rho}\tilde{u}, \quad \overline{\rho}\tilde{v}, \quad \overline{\rho}\tilde{e}, \quad \overline{\rho}\tilde{Y}_k\right]^T \tag{2}$$

$$\mathbf{E} = y\left[\overline{\rho}\tilde{u}, \quad \overline{\rho}\tilde{u}^2 + \overline{p}, \quad \overline{\rho}\tilde{u}\tilde{v}, \quad (\overline{\rho}\tilde{e} + \overline{p})\tilde{u}, \quad \overline{\rho}\tilde{u}\tilde{Y}_k\right]^T \tag{3}$$

$$\mathbf{F} = y\left[\overline{\rho}\tilde{v}, \quad \overline{\rho}\tilde{u}\tilde{v}, \quad \overline{\rho}\tilde{v}^2 + \overline{p}, \quad (\overline{\rho}\tilde{e} + \overline{p})\tilde{v}, \quad \overline{\rho}\tilde{v}\tilde{Y}_k\right]^T \tag{4}$$

where the overbar and tilde = time- and Favre-averaged quantities, respectively. The superscript T stands for the transpose of the vector. Standard notations in fluid mechanics are used. The formulation is closed by the equation of state for a perfect mixture

$$\overline{p} = \overline{\rho} R_u \overline{T} \sum_{k=1}^{N} \frac{\tilde{Y}_k}{W_k} \tag{5}$$

where R_u = universal gas constant; and W_k = molecular weight of species k.

Turbulence closure is achieved using the low-Reynolds-number κ-ε two-equation model of Yang and Shih (1993), which has demonstrated its accuracy and efficiency in treating complex flows

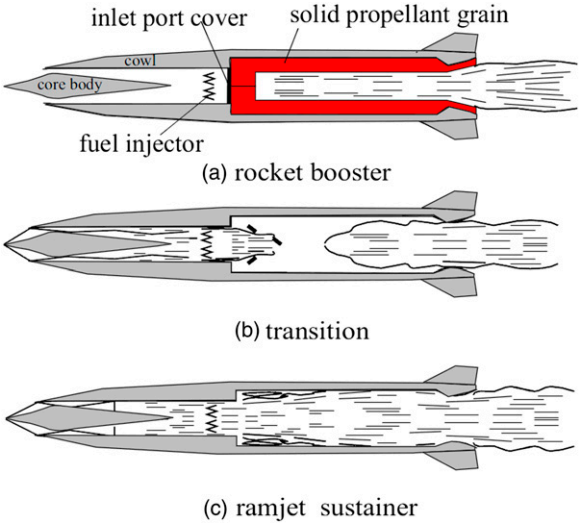

Fig. 1. Schematic diagram of a coaxial IRR engine during the transition from the rocket booster to the ramjet sustainer phase: (a) rocket booster; (b) transition; (c) ramjet sustainer

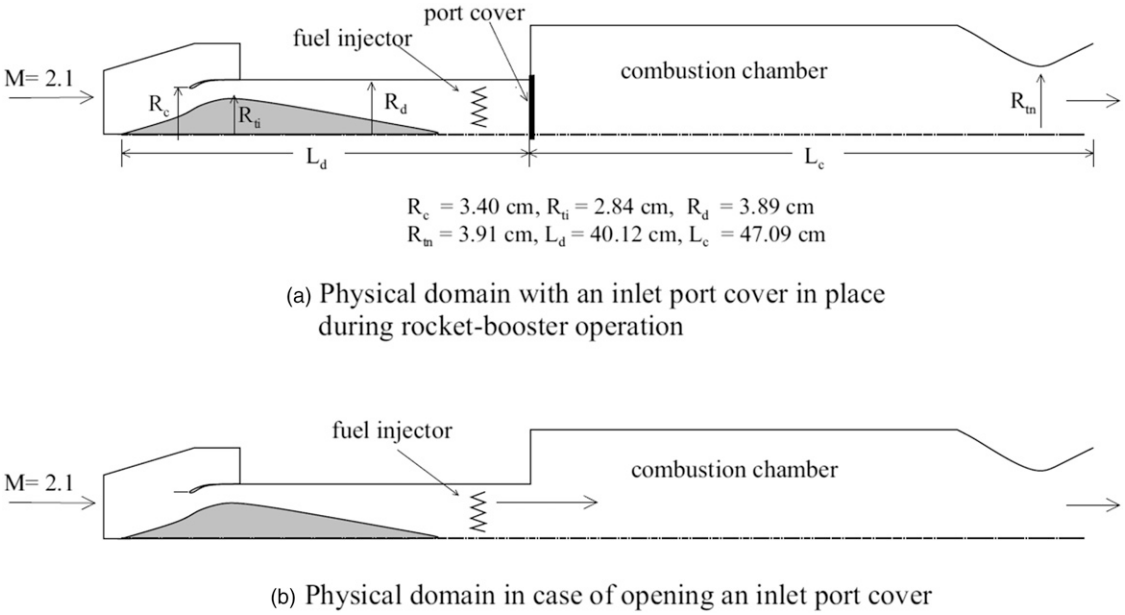

Fig. 2. Physical geometries with and without inlet port cover in the booster and sustainer phases, respectively: (a) physical domain with inlet port cover in place during rocket booster operation; (b) physical domain during ramjet sustainer operation

J. Aerosp. Eng. 2014.27:390-397.

over a wide range of Reynolds numbers. The approach includes a time scale–based k-ε model for the near-wall turbulence to avoid the singularity at the wall. Adaptation to separated flows is made by using a damping function based on the Reynolds number instead of y^+. The model is designed to maintain the high Reynolds number formulation in the logarithmic law region and is further tuned to fit experimental data for the viscous and buffer layers.

The one-step global kinetics scheme proposed by Westbrook and Dryer (1981) is adopted in light of its simplicity and reasonably accurate modeling of hydrocarbon flames in air. The overall reaction mechanism for the combustion of hydrocarbon fuel (C_xH_y) with air is written as

$$C_xH_y + \alpha(O_2 + 3.76N_2) \rightarrow xCO_2 + (y/2)H_2O + \beta O_2 + 3.76\alpha N_2 \tag{6}$$

where the coefficients α and β are determined by the fuel formula and mixture composition. The reaction rate of the fuel takes the following Arrhenius form:

$$\dot{\omega}_{C_xH_y} = AT^m \exp\left(-\frac{E}{R_uT}\right)[C_xH_y]^a[O_2]^b \tag{7}$$

The consumption rates of other species can be obtained from the overall reaction mechanism [Eq. (6)]. In this study, propane (C_3H_8) is selected as a fuel. The frequency factor A is 1.42×10^{11} $m^3/kmol{\cdot}s$, and the activation energy E is 125.52 kJ/mol (30 kcal/mol). The exponents a, b, and m have values of 0.1, 1.65, and 0, respectively (Zarlingo 1988). The unit of $\dot{\omega}_{CxHy}$ is kg/m^3s.

Physical Domain and Boundary Conditions

Fig. 2 shows the IRR engine under consideration, consisting of an axisymmetric mixed-compression supersonic inlet, a dump combustion chamber, a fuel injection unit, a port cover, and an exhaust nozzle. The projected cowl radius R_c is 3.4 cm, and the length of the inlet diffuser is 40.12 cm. The combustion chamber measures 38.93 cm in length and 7.786 cm in radius, and the nozzle length is 8.16 cm. The throat area of the inlet diffuser A_{ti} is fixed at 0.615 A_c and that of the exhaust nozzle A_{tn} at 1.322 A_c, where A_c is the projected area of the cowl, $A_c \equiv \pi R_c^2$. Detailed information about the cowl and center body geometries is given in Oh et al. (2005). The freestream conditions include a Mach number of 2.1 and an altitude of 2.5 km. The corresponding temperature and pressure are 272 K and 74.98 kPa, respectively, and the stagnation temperature and pressure are 512 K and 6.77 atm, respectively.

To facilitate the analysis of the flow transients during the transition from the booster to the sustainer phase, two different computational geometries are considered. One consists of the inlet diffuser and the booster combustion chamber, separated by the inlet port cover [Fig. 2(a)], and the other includes the entire ramjet flow path without the port cover [Fig. 2(b)]. The computational domain is divided into four zones, as shown in Fig. 3. Zone 1 is the external flow region and contains 88×50 cells. Zone 2 covers the supersonic inlet diffuser and has 214×60 cells. The combustion chamber contains Zones 3 and 4, involving 170×60 and 170×50 cells, respectively. The grids are clustered in regions with steep gradients to provide proper spatial resolution of the calculated flowfield.

Boundary conditions are specified according to the method of characteristics. Because the inflow is supersonic, the flow variables at the upstream boundary are fixed at their corresponding freestream conditions. At the exit, the flow is also supersonic, after it passes through the choked exhaust nozzle. The flow variables can thus be obtained by extrapolating from the interior points. All the solid walls are assumed to be adiabatic and nonslip, with the velocities and the normal gradients of other flow variables set to zero. Flow symmetry is enforced along the centerline. Finally, the flow variables at the far-field boundary are extrapolated from the interior along the characteristic lines, based on the solution of a simple wave (Roache 1982), to avoid shock reflections.

Numerical Method and Model Validation

The theoretical formulation outlined previously was solved numerically by means of a density-based, finite-volume methodology. The current study features a wide variation of the flow velocity in the engine flowpath. The Mach number ranges from 2.1 in the freestream to a low value in the dump combustor. The resulting disparity of the eigenvalues of the governing equations may cause serious numerical stiffness and convergence problems. To overcome this difficulty, a preconditioning algorithm augmented with a dual time-stepping integration procedure is used (Hsieh and Yang 1997b). The method proceeds in two steps. First, a rescaled pressure term is used in the momentum equation to circumvent the pressure singularity problem at low Mach numbers. Second, a dual time-stepping integration procedure is established. In this study, temporal integration in the physical-time domain is obtained using a second-order backward differencing scheme, whereas the inner-loop integration in pseudo-time is achieved using the Euler implicit scheme. The spatial discretization uses the second-order upwind scheme of Chakravarthy and Osher (1985) with a minmod limiter to keep monotonic characteristics

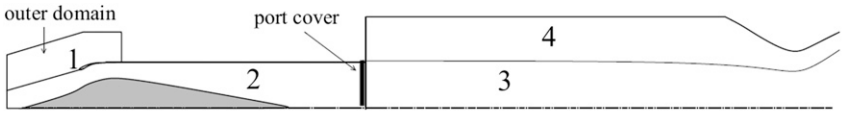

(a) Computational domain with an inlet port cover in place

(b) Computational domain in case of opening an inlet port cover

Fig. 3. Computational domains for cases with and without inlet port cover: (a) computational domain with an inlet port cover in place; (b) computational domain in case of opening an inlet port cover

J. Aerosp. Eng. 2014.27:390-397.

for convective terms and a second-order central differencing scheme for viscous terms. Finally, the alternating-direction-implicit scheme is used to treat the discretized governing equations in the block penta-diagonal matrix form. The overall algorithm was optimized to minimize the computational time and memory requirements.

The numerical approach has been validated against a variety of flow problems to assess its accuracy. These include the aerodynamics in an isentropic compression inlet (Hsieh and Yang 1997a), shock/acoustic wave interactions (Yang and Culick 1985), solid-propellant rocket motor interior flows (Roh et al. 1995), and flow instabilities in porous chambers (Apte and Yang 2003). In each of these studies, good agreement was obtained with either analytical solutions or experimental data.

Flow Transients from Booster to Sustainer

Analysis was first conducted to determine the combustor pressure after the burnout of the booster rocket propellant. Fig. 4 shows the temporal evolution of the pressure measured at the corner behind the dump plane. The pressure decreases exponentially from 40 to 3 atm during the tail-off of the booster phase. The port cover at the combustor entrance bursts at $t = 0$ ms and is then expelled downstream through the chamber to the ambient environment. Fuel injection immediately follows at 1 ms. Ignition is achieved in the corner recirculation region in the combustor at 2.5 ms using a heat source. The flame spreads outward and soon reaches its steady-state condition with a chamber pressure of around 5.5 atm.

Flow Fields with Inlet Port Cover in Place

During the booster phase, the combustion chamber functions as a conventional rocket motor. The inlet diffuser is isolated from the combustor by a port cover at the interface, as depicted in Fig. 2(a), and acts as a coaxial cavity filled with stagnant air. This geometric division allows the flowfields in the inlet diffuser and rocket combustor to be calculated separately. Results are used as the initial conditions for calculating the internal flow evolution in the sustainer phase.

Fig. 5 shows the streamlines and the Mach number distributions in the inlet diffuser and the external flow region around the cowl. Air approaches the engine at a Mach number of 2.1, passes through a shock train in the compression section, and becomes stagnant downstream of the center body, because of the presence of the port cover at the interface with the rocket combustion chamber. Fig. 6 shows the detailed flow development near the inlet entrance. The normal shock wave stemming from the center body intersects the two oblique shocks originating from the leading cone and leads to the development of a strong bow shock extending into the external flow region. Because of the air stagnation within the inlet diffuser, all the approaching air must be diverted and spilled over the inlet to the ambient environment, as indicated by the rapid change of flow direction near the cowl lip [Fig. 6(a)]. A separation bubble is observed on the outer surface of the cowl. In addition, a small lambda shock wave is present on the center body surface, because of the interactions between the normal shock wave and boundary layer. The flow phenomena in this region are very complicated, involving a series of compression and expansion processes, shock intersections, vortex formation, viscous interactions, and flow diversion, as shown schematically in Fig. 7.

Flow Fields after Removal of Inlet Port Cover

Fig. 8 shows the evolution of the Mach number field in the entire engine flowpath during the time span from $t = 0$ (removal of the inlet cover) to 2.5 ms (ignition of the fuel). A more detailed history of the flow in the inlet is given in Fig. 9. Soon after the removal of the inlet port cover at $t = 0$ ms, the pressure at the inlet exit decreases abruptly. The compressed ram air initially stagnant in the inlet diffuser enters the combustor and purges the residual combustion products of the booster solid propellant out of the chamber. The inlet begins to

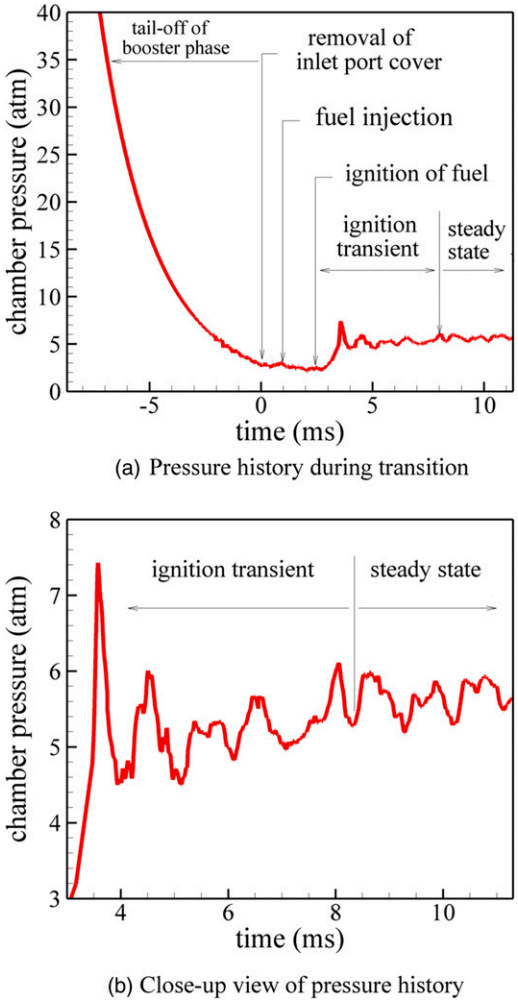

Fig. 4. Time history of combustor pressure during transition from booster to sustainer phase: (a) pressure history during transition; (b) close-up view of pressure history

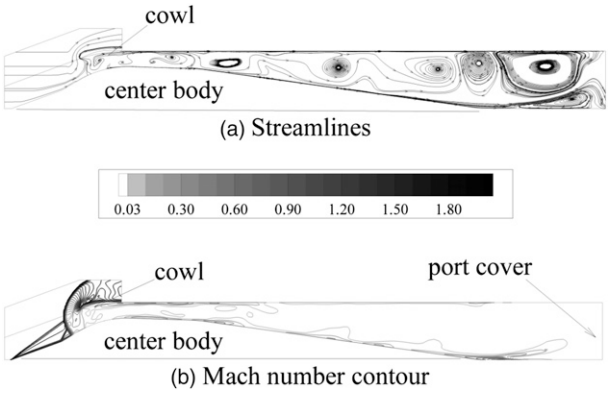

Fig. 5. Flowfield in inlet diffuser with port cover in place at exit: (a) streamlines; (b) Mach number contour

J. Aerosp. Eng. 2014.27:390-397.

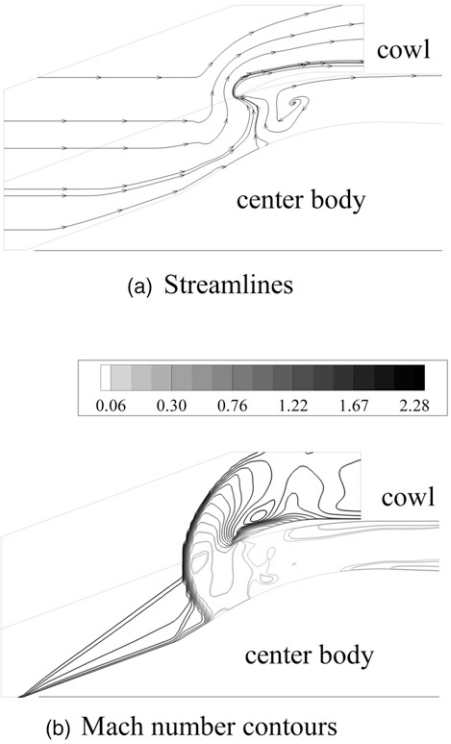

Fig. 6. Close-up view of flowfield near inlet entrance: (a) streamlines; (b) Mach number contours

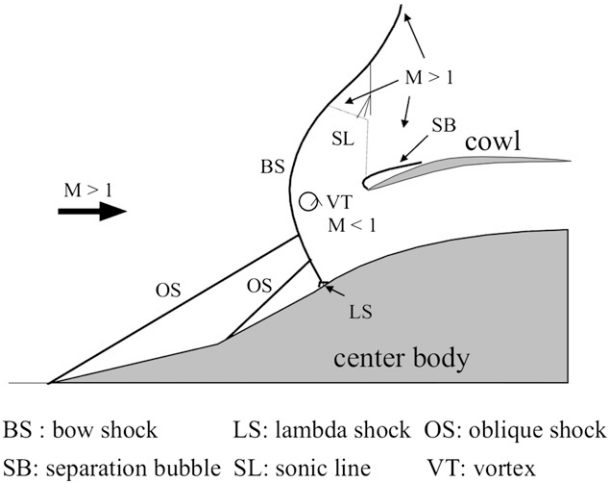

Fig. 7. Schematic of flow field near cowl lip prior to removal of inlet port cover

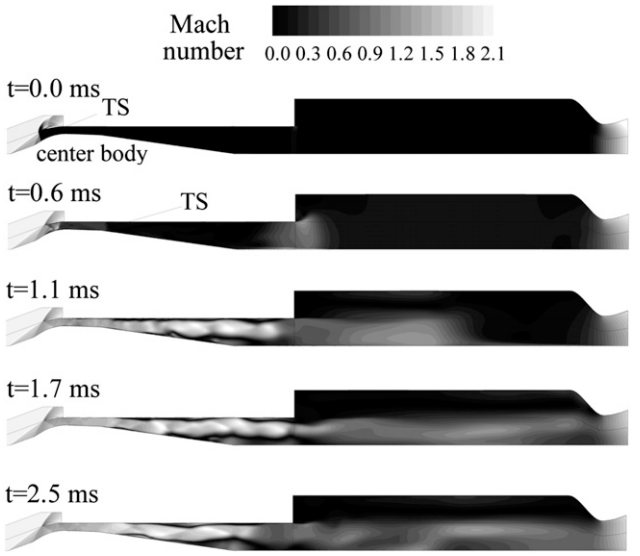

Fig. 8. Temporal evolution of Mach number field in the entire ramjet engine after the removal of the inlet port cover

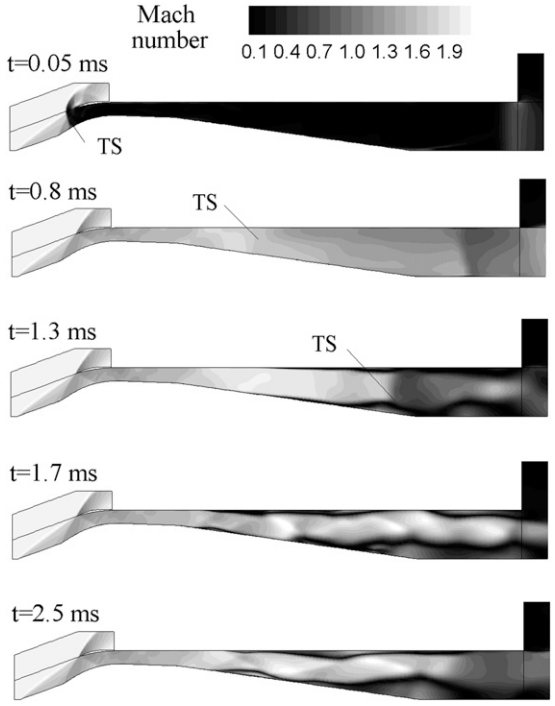

Fig. 9. Time evolution of Mach number field in inlet after removal of inlet port cover

inhale the approaching air. As a result, the terminal normal shock wave in front of the cowl moves downstream and finally dissipates at 1.7 ms. The flow is predominantly supersonic in both the inlet diffuser and combustor. Fig. 10 shows the evolution of the flow structure in the combustor. A large recirculation flow exists in the expanded region of the combustor. The embedded vortices oscillate in size like unsteady bubbles pressurized by the main stream, as evidenced by the streamlines shown in Fig. 10.

It is worth noting that the fuel should be injected into the combustor immediately after the inlet port cover is ruptured and, most importantly, prior to the establishment of a supersonic flow throughout the main flow passage in the combustor. Otherwise, the fuel may not be efficiently entrained into the corner recirculation zone in the combustor, and ignition failure may result. The combustor streamlines shown in Fig. 10 suggest that the time instant of 1.0 ms appears to be appropriate for the onset of fuel injection in the present case, to allow the fuel to penetrate into the recirculation zone.

Fig. 11 shows the temporal evolution of the temperature field in the combustor. After the propellant burnout at the end of the booster phase, the combustor gases expand isentropically until the removal of the port cover at $t = 0$ ms, at which point the chamber temperature

J. Aerosp. Eng. 2014.27:390-397.

and pressure reach 1,350 K and 3.1 atm, respectively. The ram air then enters rapidly into the chamber and mixes with the combustion products of the booster propellant, further reducing the chamber pressure at the dump plane to 2.8 atm and the temperature to 1,230 K at $t = 1.7$ ms. The decrease in the temperature near the entrance of the exhaust nozzle at $t = 0.8$ ms results from the continuous depressurization of the propellant combustion products through the nozzle. Although the ram air displaces most of the propellant products, a small amount of hot gas still remains in the corner recirculation zone and near the combustor wall. The former may play an important role in determining the ignition behavior in the transition phase. This phenomenon will be discussed later.

Based on the previous observations, three potentially positive mechanisms to assist stable ignition of the ramjet fuel are identified. First, the expansion of the ram air enhances the spreading of fuel into the recirculation zone. Second, even after the introduction of the cold ram air into the chamber, some high-temperature gas still remains downstream of the backward-facing step to supply thermal energy to ignite the fuel. Finally, the relatively uniform temperature in the chamber helps reduce pressure spikes because of irregular ignition of reactants by local hot spots.

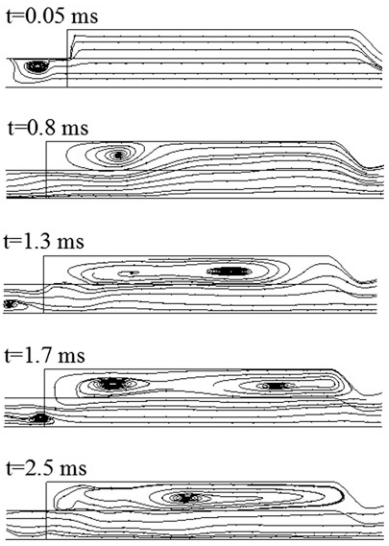

Fig. 10. Time evolution of streamlines in combustor after removal of inlet port cover

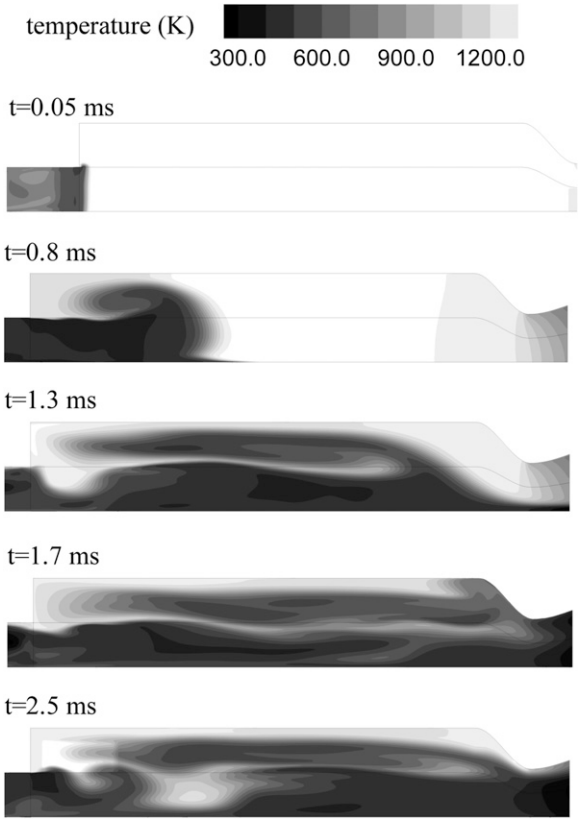

Fig. 11. Temporal evolution of temperature field prior to ignition

Ignition and Flame Development

Efficient and reliable ignition of the fuel/air mixture during the booster-to-sustainer transition represents a critical issue in the development of an IRR engine. Ignition must be achieved in the shortest possible time interval with a minimal requirement of energy input. Overpressurization resulting from fuel accumulation and an exceedingly large ignition source must be avoided to prevent system failure. Thus, the spatial locations of the igniter and fuel injector and the timing of the operation sequence need to be carefully optimized.

In the current study, propane (C_3H_8) fuel with a mass flow rate of $0.12\,\mathrm{kg/s}$ is uniformly injected over the flow passage at 4 cm upstream of the dump plane. The overall equivalence ratio of the fuel/air mixture is 0.8. The injector orifices are choked to maintain a fixed mass flow rate and eliminate influence from the surrounding flow conditions. Fig. 12 shows the temporal evolution of the fuel mass fraction distribution in the combustor. The fuel injection commences at $t = 1$ ms. As expected, the fuel stream follows the cold ram air because of the rapid fuel/air mixing near the injectors. Initially, the flow expansion near the dump plane facilitates the penetration of fresh reactants into the corner recirculation zone. The vortical motions in the shear layer originating from the edge of the backward-facing step (as shown in Fig. 13) then provides the mechanism for

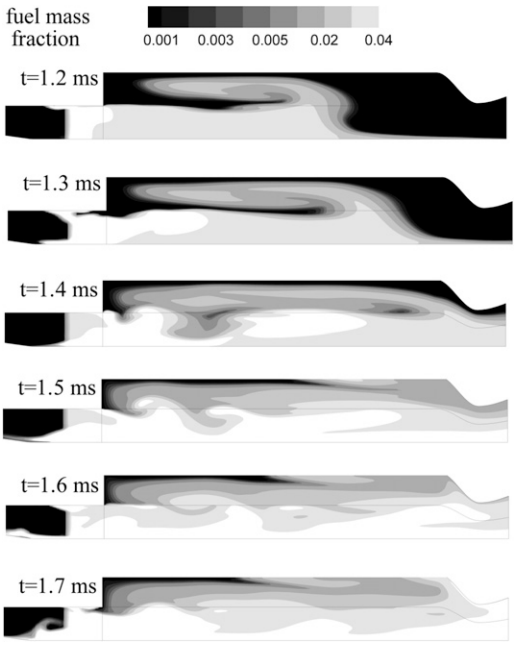

Fig. 12. Temporal evolution of fuel mass fraction field prior to ignition

J. Aerosp. Eng. 2014.27:390-397.

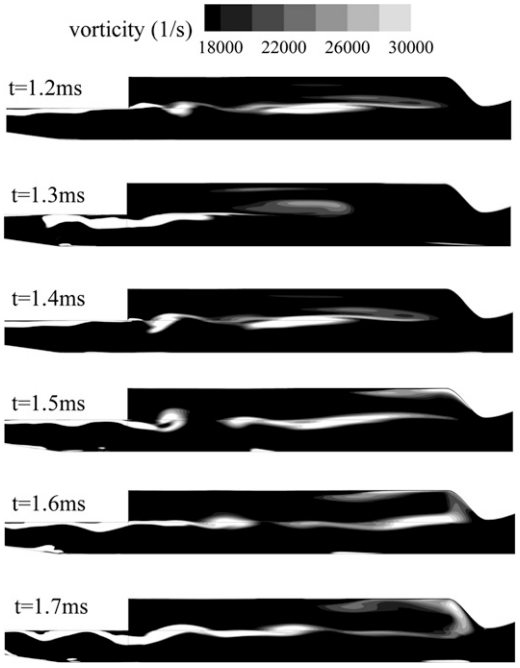

Fig. 13. Temporal evolution of vorticity field prior to ignition

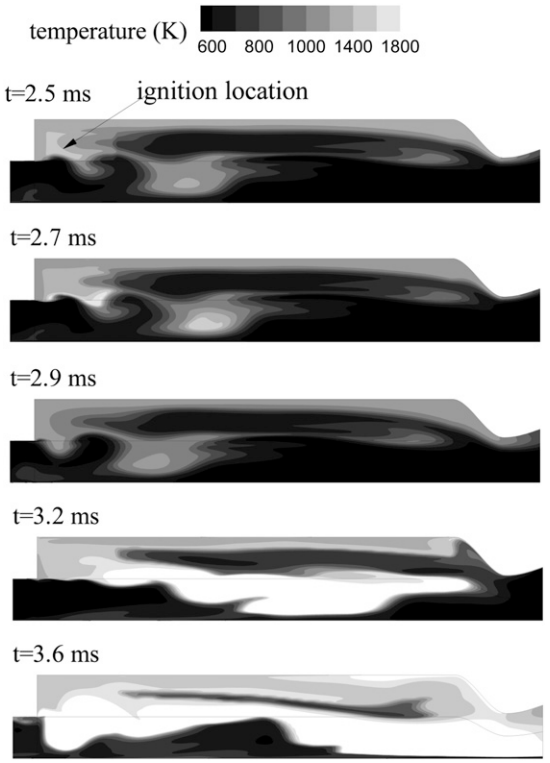

Fig. 14. Temporal evolution of temperature field in combustor during ignition transient

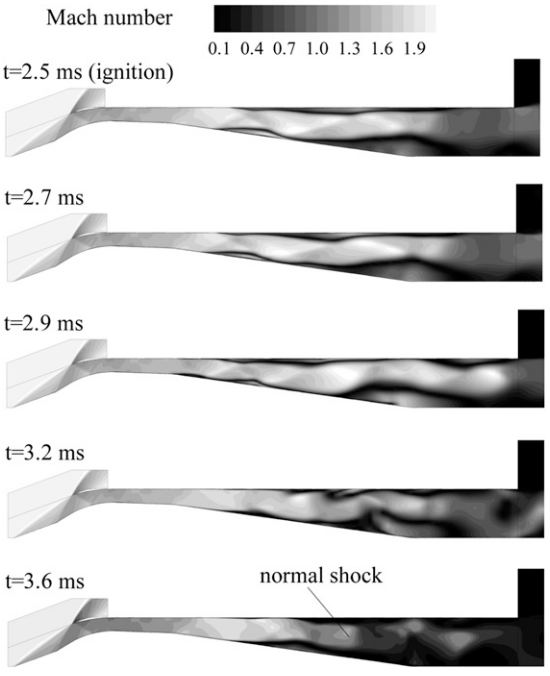

Fig. 15. Temporal evolution of Mach number field in inlet during ignition transient

mixing the cold reactants and the hot product gases produced in the booster phase. The fuel distribution is highly uniform in the chamber during the transition phase. A small amount of fuel is found in regions upstream of the injector, mainly because of the flow unsteadiness and separation in the inlet diffuser.

To ignite the reactants, a heat source is supplied at $t = 2.5$ ms in the corner region behind the dump plane, until the local gas temperature reaches the autoignition point of the fuel/air mixture. Fig. 14 shows the temperature evolution in the combustor during the ignition transient. The incoming ram air temperature is 571 K, and the Mach number at the inlet exit is 0.79. The hot spot around 1,500 K at 2.5 ms corresponds to the ignition location, and the high-temperature regions (~1,200 K) near the wall and around the centerline are associated with the residual combustion products of the booster propellant. The flame propagates rapidly in regions with an appropriate equivalence ratio and velocity. The flame speed depends on the local temperature, pressure, equivalence ratio, turbulence level, and convective velocity. A more detailed description of the flame propagation mechanisms is given in the companion paper (Sung and Yang 2014).

Fig. 15 shows the temporal evolution of the Mach number field in the inlet, with each frame synchronized with the snapshot of the temperature field shown in Fig. 14. As discussed in the previous section, "Flow Fields after Removal of Inlet Port Cover," the flowfield in the inlet diffuser is predominantly supersonic after the removal of the port cover, mainly because of the low pressure (~3 atm) in the combustor prior to ignition. Flow separation occurs in the downstream section of the center body and causes a low-speed recirculating flow along the centerline. The information regarding the pressure rise caused by ignition in the combustor can propagate only through the subsonic regions near the walls. The resultant adverse pressure gradient enhances flow separation and subsequently reduces the effective supersonic flow passage area in the inlet. As a consequence, the peristalsis of the supersonic core becomes stretched, segregated, and even strengthened at $t = 2.9$ ms. The increased combustor pressure reduces the flow velocity in the inlet. At $t = 3.2$ ms, the velocity at the inlet exit becomes largely subsonic. A terminal shock forms soon afterward and further exacerbates the flow separation in the divergent section of the inlet diffuser. The subsonic region, however, continues to grow and leads to the formation of a terminal normal shock wave at $t = 3.6$ ms. The pressure spike of 7.4 atm at 3.6 ms in Fig. 4 arises from the burning of the reactants

J. Aerosp. Eng. 2014.27:390-397.

accumulated in the chamber prior to the arrival of the flame. As the flame develops in the combustor, the chamber pressure increases and eventually reaches its design condition of 5.5 atm for ramjet operation.

Summary and Conclusions

The transition from the rocket booster to the ramjet sustainer phase of an IRR engine was numerically investigated by treating the conservation equations for a multicomponent chemically reacting system. The model takes into account finite-rate chemical kinetics and uses a low-Reynolds-number κ-ε turbulence scheme. The computational geometry consists of the entire engine flowpath, from the freestream in front of the inlet through the exit of the exhaust nozzle.

The flowfields in the inlet diffuser and combustion chamber were first obtained with the port cover in place at the entrance of the combustor. Immediately on the removal of the port cover, the ram air entered the combustor at a supersonic speed. Fuel injection and ignition then followed. The ensuing flame establishment increased the chamber pressure to its design value for ramjet operation. Concurrently, the flowfield in the inlet diffuser started to settle down, and eventually a terminal normal shock wave formed and was sustained in the divergent section of the inlet diffuser. The operation timing played an important role in achieving robust ignition and flame development.

References

Apte, S., and Yang, V. (2003). "A large eddy simulation study of transition and flow instability in a porous-walled chamber with mass injections." *J. Fluid Mech.*, 447(2), 215–225.

Barber, T., Maicke, B., and Majdalani, J. (2009). "Current state of high speed propulsion: Gaps, obstacles and technological challenges in hypersonic applications." *AIAA Paper 09-5118, 45th AIAA/ASME/SAE/ASEE Joint Propulsion Conf.*, American Institute of Aeronautics and Astronautics (AIAA), Reston, VA.

Bemdot, J. G., Heins, A. E., and Piercy, T. G. (1984). "Ramjet air induction system for tactical missile application." *AGARD-LS-136*, Marquardt Company, Van Nuys, CA, 2.1–49.

Bogar, T. J., Sajben, M., and Kroutil, J. C. (1985). "Response of supersonic inlet to downstream perturbations." *J. Propul. Power*, 1(2), 118–125.

Chakravarthy, S. R., and Osher, S. (1985). "A new class of high accuracy TVD schemes for hyperbolic conservation laws." *AIAA Paper 85-0363, 23rd AIAA Aerospace Science Meeting*, American Institute of Aeronautics and Astronautics (AIAA), Reston, VA.

Fry, R. S. (2004). "A century of ramjet propulsion technology evolution." *J. Propul. Power*, 20(1), 27–38.

Fung, Y. T., and Yang, Y. (1992). "Active control of nonlinear pressure oscillation in combustion chambers." *J. Propul. Power*, 8(6), 1282–1289.

Fung, Y. T., Yang, Y., and Sinha, A. (1991). "Active control of combustion instabilities with distributed actuators." *Combust. Sci. Technol.*, 78(4–6), 217–245.

Hsieh, S., and Yang, V. (1997a). "A unified analysis of unsteady flow structures in a supersonic ramjet engines." *AIAA Paper 97–0396, 35th AIAA Aerospace Science Meeting*, American Institute of Aeronautics and Astronautics (AIAA), Reston, VA.

Hsieh, S. Y., and Yang, V. (1997b). "A preconditioned flux-differencing scheme for chemically reacting flows at all mach numbers." *Int. J. Comput. Fluid Dyn.*, 8(1), 31–49.

Hsieh, T., Bogar, T. J., and Coakley, T. J. (1987). "Numerical simulation and comparison with experiment for self-excited oscillations in a diffuser flow." *AIAA J.*, 25(7), 936–943.

Lu, P., and Jain, L. (1998). "Numerical investigation of inlet buzz flow." *J. Propul. Power*, 14(1), 90–100.

Matveev, K., and Culick, F. (2003). "A model for combustion instability involving vortex shedding." *Combust. Sci. Technol.*, 175(6), 1059–1083.

Menon, S., and Jou, W.-H. (1991). "Large-eddy simulations of combustion instability in an axisymmetric ramjet combustor." *Combust. Sci. Technol.*, 75(1–3), 53–72.

Myers, T. D. (1984). "Integral boost, heat protection, port covers and transition." *AGARD-LS-136,* United Technologies Chemical Systems Division, San Jose, CA, 4.1–20.

Oh, J. Y., Ma, F., Hsieh, S. Y., and Yang, V. (2005). "Interactions between shock and acoustic waves in a supersonic inlet diffuser." *J. Propul. Power*, 21(3), 486–495.

Ristori, A., Heid, G., Brossard, C., and Bresson, A. (2003). "Characterization of the reacting two-phase flow inside a research ramjet combustor." *ONERA TP No. 2003-145*, ONERA, Chatillon, France.

Roache, P. J. (1982). *Computational fluid dynamics*, Hermosa Publishers, Albuquerque, NM, 282–283.

Roh, T. S., Tseng, I. S., and Yang, V. (1995). "Effect of acoustic oscillations on flame dynamics of homogeneous propellants in rocket motors." *J. Propul. Power*, 11(4), 640–650.

Sung, H.-G., and Yang, V. (2014). "Unified analysis of internal flowfield in an integrated rocket ramjet engine. II: Ramjet sustainer." *J. Aerosp. Eng.*, 10.1061/(ASCE)AS.1943-5525.0000256, 398–403.

Waltrup, P. J., White, M. E., and Gravlin, E. S. (2002). "History of U.S. Navy ramjet, scramjet, and mixed-cycle propulsion development." *J. Propul. Power*, 18(1), 14–27.

Webster, F. F. (1989). "Ramjet development testing: Which way is right?" *J. Propul. Power*, 5(5), 565–576.

Westbrook, C. K., and Dryer, F. L. (1981). "Simplified reaction mechanisms for the oxidation of hydrocarbon fuels in flames." *Combust. Sci. Technol.*, 27(1–2), 31–43.

Yang, V., and Culick, F. E. C. (1985). "Analysis of unsteady inviscid diffuser flow with a shock wave." *J. Propul. Power*, 1(3), 222–228.

Yang, V., and Culick, F. E. C. (1986). "Analysis of low frequency combustion instabilities in a laboratory ramjet combustor." *Combust. Sci. Technol.*, 45(1), 1–25.

Yang, Z., and Shih, T. H. (1993). "New time scale based k-ε model for near-wall turbulence." *AIAA J.*, 31(7), 1191–1197.

Zarlingo, F. (1988). "Airbreathing propulsion concepts for high speed tactical missiles." *AIAA Paper 1988–3070, 24th AIAA/ASME/SAE/ASEE Joint Propulsion Conf.*, American Institute of Aeronautics and Astronautics (AIAA), Reston, VA.